

Catalytic Disproportionation of Hydrogen Peroxide by the Tetranuclear Manganese Complex $[\text{Mn}^{\text{II}}(2\text{-OHpicpn})_4]$

Andrew Gelasco, Anke Askenas, and Vincent L. Pecoraro*

Department of Chemistry, The University of Michigan, Ann Arbor, Michigan 48109-1055

Received August 9, 1995

Manganese enzymes containing dinuclear or tetranuclear active sites often catalyze the disproportionation of H_2O_2 to H_2O and O_2 .¹ Recently we^{2,3} and others⁴ reported functional dinuclear models for the Mn catalases and the alternative catalase reaction for the OEC. In addition, a manganese complex that is tetranuclear in the solid state has been shown to disproportionate H_2O_2 in water at a rate faster than uncomplexed Mn^{II} ion, an observation that is consistent with a multinuclear reaction site.⁵ Herein we report a tetranuclear Mn complex that catalytically disproportionates H_2O_2 using the ligand 2-OHpicpn.

The reaction of $\text{Mn}^{\text{II}}(\text{ClO}_4)_2 \cdot 6\text{H}_2\text{O}$ (0.181 g; 0.5 mmol) with 2-OHpicpn (0.134 g; 0.5 mmol) and 1 equiv of NaOMe in methanol yields a tan powder which can be recrystallized from acetonitrile to give orange crystals of $[\text{Mn}^{\text{II}}(2\text{-OHpicpn})_4](\text{ClO}_4)_4$, **1**.⁶ This complex has been crystallographically characterized as the hexakis(acetonitrile) solvate, $\mathbf{1} \cdot 6\text{CH}_3\text{CN}$, confirming the proposed tetranuclear structure.⁷ An ORTEP diagram of the cation is shown in Figure 1.

The manganese ions are spanned by monoalkoxide bridges, with an average Mn–Mn distance of 3.74 Å. Each Mn coordination sphere contains one pyridine nitrogen, one imine nitrogen, and one alkoxide oxygen, each from two different ligands, in a rhombically distorted octahedron. The pyridine nitrogen–manganese bonds are the longest of the ligand–metal bonds (2.40 Å average bond length) and are trans to the short

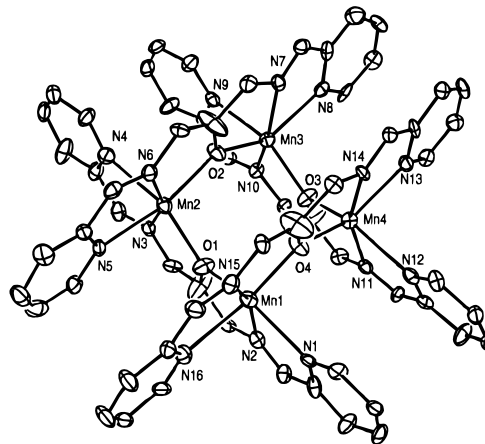


Figure 1. ORTEP diagram of the cation $[\text{Mn}_4(2\text{-OHpicpn})_4]^{4+}$, **1**: Mn1–Mn2 3.750 Å, Mn1–Mn4 3.716 Å, Mn2–Mn3 3.765 Å, Mn3–Mn4 3.713 Å. Average bond lengths (range in parentheses): Mn– N_{py} 2.40 (± 0.03) Å, Mn– N_{imine} 2.22 (± 0.02) Å, Mn– O_{alk} 2.11 (± 0.01) Å. Representative angles: Mn1–O1–Mn2 99.1(1)°, O1–Mn1–O4 104.7(4)°, O1–Mn1–N1 145.6(4)°, O1–Mn1–N2 75.8(4)°, O1–Mn1–N15 114.9(4)°, O1–Mn1–N16 92.2(4)°, N2–Mn1–N16 90.3(4)°, O4–Mn1–N190.0(3)°, O4–Mn1–N2 121.6(4)°, O4–Mn1–N15 75.9(4)°, O4–Mn1–N16 146.5(4)°, N1–Mn1–N2 70.1(4)°, N1–Mn1–N15 98.7(4)°, N1–Mn1–N16 92.0°, N2–Mn1–N15 158.0(3), N15–Mn1–N16 70.8(4).

- (1) (a) Penner-Hahn, J. E. In *Manganese Redox Enzymes*; Pecoraro, V. L., Ed.; VCH Publishers: New York, 1992; pp 29–45. (b) Waldo, G. S.; Penner-Hahn, J. E. Submitted to *Biochemistry*. (c) Cavalli, R. C.; Burke, C. J.; Soprano, D. R.; Kawamoto, S.; Ash, D. E. Submitted to *Biochemistry*. (d) Frasc, W. D.; Mei, R. *Biochemistry* **1987**, 26, 7321–7325.
- (2) Gelasco, A.; Pecoraro, V. L. *J. Am. Chem. Soc.* **1993**, 115, 7928–7929.
- (3) Larson, E. J.; Pecoraro, V. L. *J. Am. Chem. Soc.* **1991**, 113, 7809–7810.
- (4) (a) Bossek, U.; Saher, M.; Weyhermuller, T.; Wieghardt, K. *J. Chem. Soc., Chem. Commun.* **1992**, 1780–1782. (b) Sakiyama, H.; Okawa, H.; Isobe, R. *J. Chem. Soc., Chem. Commun.* **1993**, 882–884. (c) Mathur, P.; Crowder, M.; Dismukes, G. C. *J. Am. Chem. Soc.* **1987**, 109, 5227–5233. (d) Pessiki, P. J.; Dismukes, G. C. *J. Am. Chem. Soc.* **1994**, 116, 898–903.
- (5) Stibrany, R. T.; Gorun, S. M. *Angew. Chem., Int. Ed. Engl.* **1990**, 29, 1156–1158.
- (6) Anal. Calcd for **1**, $\text{Mn}_4\text{C}_{60}\text{H}_{60}\text{N}_{16}\text{O}_{20}\text{Cl}_4$: C, 53.4; H, 4.49; N, 6.93; Mn, 13.59. Found: C, 53.1; H, 4.67; N, 6.89; Mn, 13.6. Yield: 0.76 g; 91% based on tetramer. ESI+ spectrum gives molecular ion peak (m/e) for $[\text{Mn}_4(2\text{-OHpicpn})_4](\text{ClO}_4)_3^+$ at 1587.5 and other peaks at 744 ($[\text{Mn}_4(2\text{-OHpicpn})_4](\text{ClO}_4)_2^{2+} = 1487.9$; ESI-MS shows 1487.9/2 = 744) with the isotope pattern consistent only for two perchlorates. Room-temperature $\mu_{\text{eff}} = 5.04 \mu_{\text{B}}/\text{Mn}$.
- (7) X-ray parameters for **1**· $6\text{CH}_3\text{CN}$: $[\text{Mn}_4(2\text{-OHpicpn})_4](\text{ClO}_4)_4 \cdot 6\text{CH}_3\text{CN}$, $\text{Mn}_4\text{C}_{72}\text{H}_{78}\text{N}_{22}\text{O}_{20}\text{Cl}_4$, MW 1933.14; crystal system triclinic P1 (No. 2); $a = 14.044(9)$, $b = 14.18(1)$, $c = 22.67(2)$ Å; $\alpha = 79.36(5)$, $\beta = 73.77(5)$, $\gamma = 89.55(6)^\circ$; $V = 4263(5)$ Å³; $Z = 2$; $d_{\text{obsd}} = 1.69$, $d_{\text{calcd}} = 1.68$ g/cm³; crystal dimensions $0.21 \times 0.22 \times 0.15$ mm; Mo K α (0.7107 Å); $T = 145$ K; Siemens R3m/v four-circle diffractometer; data reduced using the SHELXTL PLUS program package, on a VAXstation 3500. All non-hydrogen atoms, except one perchlorate oxygen and three methylene carbon atoms, were refined anisotropically. Hydrogen atoms were placed, with positional parameters using a riding model, and $U = 0.08$ Å². $\mu = 7.8$ cm⁻¹; $4 < 2\theta < 45^\circ$; number of unique reflections = 11 109, number of parameters = 1093 (in approximately two equal blocks); number of reflections with $I > 3\sigma(I) = 7686$; GOF = 1.467, $R = 0.0978$, $R_w = 0.103$.

(2.11 Å) manganese–alkoxide bonds. The imine nitrogens are trans to one another, with intermediate bond lengths of 2.22 Å. Selected bond lengths and angles for this complex are contained in the caption to Figure 1.

If **1** is dissolved in acetonitrile at concentrations greater than 25 μM , the complex remains a tetramer. This assignment is supported by electrospray ionization mass spectrometry (ESI-MS). Analysis of the higher concentration solutions showed a mass peak in the ESI-MS⁺ spectrum at m/e 1587.5 consistent with the tetramer tetracation and three perchlorate anions. The 77 K EPR spectrum of **1** in acetonitrile/dichloromethane is characterized by a $g = 2$ resonance that is nearly 2200 G in width.⁸ This spectrum is consistent with a coupled Mn^{II} cluster; however, the complex is EPR silent at 5 K, whereas mononuclear Mn(II) is EPR active. There is no evidence for monomeric Mn^{II} even at a 100 μM concentration.

The UV–vis spectrum shows two prominent absorbance bands at 325 ($\epsilon = 51 \times 10^3 \text{ M}^{-1}\text{cm}^{-1}$) and 390 nm ($\epsilon = 48 \times 10^3 \text{ M}^{-1}\text{cm}^{-1}$) that obey Beer's law over the range of concentrations above 30 μM . Below $[\text{tetramer}] = 20 \mu\text{M}$, there is marked deviation from linear behavior, suggesting that the tetramer dissociates to lower nuclearity species. The tetramer quantitatively converts over 1000 equiv of H_2O_2 to O_2 . Isotope labeling studies (shown by GC-MS of the head gas from the reaction of **1** with a 50:50 mixture of $\text{H}_2^{16}\text{O}_2$ and $\text{H}_2^{18}\text{O}_2$ in acetonitrile) reveal that both oxygen atoms of the resulting O_2 originate from the same H_2O_2 molecule.

(8) EPR spectra were collected at 77 K. The spectrum shape was unchanged from 5 mM to 100 μM .

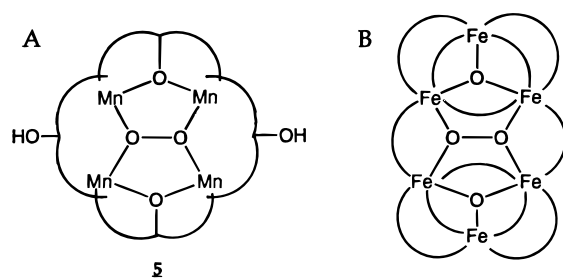


Figure 2. (A) A speculative intermediate for the $[\text{Mn}_4(2\text{-OHpicpn})_4](\text{ClO}_4)_4$ catalase reaction, **5**, based upon (B) the hexanuclear Fe complex $[\text{Fe}_6\text{O}_2(\text{O}_2)(\text{O}_2\text{CPh})_2(\text{OH}_2)_2]$ from ref 11.

We have studied the disproportionation of H_2O_2 by **1** using a Clark-type O_2 electrode to monitor initial rates of oxygen production.⁹ Complex **1** ($29\ \mu\text{M}$) exhibits saturation kinetics with hydrogen peroxide. These data can be fit to the Michaelis–Menton equation to give the kinetic parameters $V_{\text{max}} = 140 \pm 8\ \text{s}^{-1}$ and $K_{\text{M}} = 2.6 \pm 0.3\ \text{M}$. If the reaction is carried out using D_2O_2 , the V_{max} drops to $\pm 9\ \text{s}^{-1}$ and K_{M} is $3.4 \pm 0.5\ \text{M}$. The results of the H_2O_2 and D_2O_2 reactions are shown in Figure S3 (Supporting Information). The rate of this reaction has a first-order dependence on the substrate concentration at non-saturating peroxide concentrations.

The tetramer in this study has a V_{max} that is significantly higher than previously reported for any other manganese complex. However, the Michaelis constant (or effective substrate binding constant) for **1** is 2 orders of magnitude weaker than seen for the only other model complex ($[\text{Mn}(2\text{-OH}(5\text{Clisal})\text{-pn})_2]$, **2**),² for which saturation kinetics have been reported. Therefore, the catalytic efficiency ($k_{\text{cat}}/K_{\text{M}}$) of **1** ($55 \pm 9\ \text{s}^{-1}\cdot\text{M}^{-1}$) is lower than that measured for **2** ($300 \pm 13\ \text{s}^{-1}\cdot\text{M}^{-1}$). There is a similarity between **1** and **2** in that both complexes show a 50% decrease in catalytic efficiency when D_2O_2 is the substrate, illustrating that a proton-dependent step is important for the disproportionation ($29\ \text{s}^{-1}\cdot\text{M}^{-1}$ vs $120\ \text{s}^{-1}\cdot\text{M}^{-1}$ for D_2O_2).

The rate of hydrogen peroxide disproportionation also shows first-order dependence on the tetramer concentration. At tetramer concentrations above $25\ \mu\text{M}$, the rate varies linearly with catalyst concentration. The linear fit to the data has a slope of $46\ \text{s}^{-1}$, which is the first-order rate constant for the tetramer-dependent reaction at a constant $[\text{H}_2\text{O}_2]$. This value is consistent with the observed rate for $1.1\ \text{M}\ \text{H}_2\text{O}_2$ in Figure 2. These kinetic studies support the rate law shown in eq 1.

$$\text{rate} = k[\text{catalyst}][\text{H}_2\text{O}_2] \quad (1)$$

As the effective concentration of tetramer is lowered, the rate of H_2O_2 disproportionation per dissolved tetramer decreases dramatically (a plot of these data is contained in the Supporting Information). This behavior for tetramer concentrations below $25\ \mu\text{M}$ is consistent with the decomposition of the tetramer into less active or inactive species. The decomposition products must be less active than the catalyst in solution above $25\ \mu\text{M}$ because the observed rate per unit tetramer dissolved decreases rapidly.

(9) Colloidal suspensions of manganese oxides are known to disproportionate H_2O_2 . To ensure that the observed catalase reaction was not due to the formation of colloidal particles, the initially measured activity of the solution was compared to the activity of an identical solution that had been reacted with 1000 equiv of H_2O_2 and centrifuged at $25\ 000\text{g}$ for 1 h to remove all solids. An aliquot was removed and reassayed. The activities of these solutions were within 5%.

(10) Gelasco, A.; Pecoraro, V. L. Manuscript in preparation.

One possible model for this loss of activity is the formation of inactive monomeric species.

We evaluated this model by preparing the complexes $[\text{Mn}^{\text{II}}(2\text{-OHpicpnH})(\text{NCS})(\text{CH}_3\text{OH})](\text{ClO}_4)$, **3**, $[\text{Mn}^{\text{II}}(2\text{-OHpicpnH})(\text{acac})](\text{ClO}_4)$, **4**, and $[\text{Mn}^{\text{II}}(2\text{-OHpicpnH})(\text{CH}_3\text{OH})_2](\text{ClO}_4)_2$, **5**, to test the assumption that monomeric species of the 2-OHpicpn ligand would not disproportionate H_2O_2 at rates competitive with **1**. There was no evidence for O_2 production by **3**, **4**, or **5** in the presence of H_2O_2 , nor did the UV–vis spectrum change over the time frame of the catalytic reaction. A purely tetramer–monomer equilibrium does not satisfactorily model the observed kinetic data below $25\ \mu\text{M}$ in complex. The slope of the curve between 20 and $5\ \mu\text{M}$ is very steep and requires an equilibrium constant for a tetramer–monomer equilibrium of $> 10^{14}$. However, this equilibrium does not model the higher catalyst concentration data. It is probable that an equilibrium exists among tetrameric, trimeric, dimeric, and monomeric species below $25\ \mu\text{M}$. It is possible that trimers or dimers may have some catalytic activity. This would allow a less steep slope for the $5\text{--}20\ \mu\text{M}$ curve to be described by a higher equilibrium constant. The higher K_{eq} would indicate a more rapid formation of tetramer and would model the high concentration data better. While a multispecies equilibrium is possible, modeling the data with over seven parameters would be statistically unmeaningful.

Figure 2 illustrates a speculative intermediate for this catalase reaction that draws upon iron chemistry.¹¹ The reaction of **1** with H_2O_2 could lead to the protonation of two of the bridging alkoxides and concomitant binding of peroxide to the tetramer as shown by complex **6**. This intermediate is remarkably similar to Lippard's $\text{Fe}_6(\text{O}_2^{2-})$ species.¹¹ Two tetranuclear metal–peroxide complexes have been characterized crystallographically: the hexanuclear iron complex described and a Cu complex containing both a bridging peroxide and a perchlorate.¹² Starting with the coordinates of **1**, one can calculate a Mn–O distance for peroxide bound in the center of **6** using an O–O distance of $1.43\ \text{\AA}$. A reasonable Mn–O distance of $2.19\ \text{\AA}$ is obtained. The formation of such an intermediate would also be consistent with the low binding constant, the observed H/D isotope effect, and the necessity for a tetramer.

In conclusion, **1** is the first Mn complex that carries out catalase-like reactivity while retaining a tetranuclear structure. The complex is highly efficient ($V_{\text{max}} = 140\ \text{s}^{-1}$) but suffers from a poor binding constant, which may reflect significant rearrangement of bonds prior to forming the peroxo intermediate. An intermediate that is consistent with this chemistry is presented. Such a structure has been proposed as an arrangement of metals that could support water oxidation in OEC.¹¹ Clearly, four Mn ions oriented in a square motif can lead to highly efficient O_2 production from peroxide.

Acknowledgment. This work was supported by a grant from the NIH (GM39406).

Supporting Information Available: Tables containing crystal data, structure determination details, bond lengths, bond angles, anisotropic thermal parameters, positional parameters, and isotropic thermal parameters and a plot of the initial rate of peroxide disproportionation versus substrate concentration (Figure S3) (17 pages). Ordering information is given on any current masthead page.

IC951035G

(11) Micklitz, W.; Bott, S. G.; Bentsen, J. G.; Lippard, S. J. *J. Am. Chem. Soc.* **1989**, *111*, 372–374.

(12) Reim, J.; Krebs, B. *Angew. Chem., Int. Ed. Engl.* **1994**, *33*, 1969–1971.